

MEASUREMENTS INSIDE THE BLADE ROW OF A TRANSONIC COMPRESSOR WITH A TIME-OF-FLIGHT VELOCIMETER

by A. VOUILLARMET

Maître-Assistant E.C.L.

69130 Ecully, France

I. INTRODUCTION

Measurements have been done in a transonic compressor stage using a time-of-flight velocimeter. This velocimeter, built in the laboratory, has been optically adapted to the investigated machine, a new data acquisition system being studied specially for this purpose.

More than one hundred measurement points have been performed (the half of them, inside the rotating blade row). A lot of problems concerning :

- machine adaptation
- cleaning device
- seeding
- electric surroundings
- proximity of walls, and compressor geometry

have been encountered and partially solved, and are described in this paper.

II. THE COMPRESSOR CHARACTERISTICS

The compressor schematically presented figure 1 was composed of an Inlet Guide Vane, a rotor and a stator . The geometric characteristics of the rotor are :

- . hub radius : $R_h = .215 \text{ m}$
- . mean tip radius : $R_t = .270 \text{ m}$
- . number of blades : $Z = 57$

- At the design point, the compressor delivers a mass-flow rate of 15.5 kg/s with a rotating speed of 11 150 rev/mn.
- The six measurement sections are perpendicular to the shroud (three of them are, fully or partially, inside the rotating blade row).

III. THE MACHINE ADAPTATION

The compressor has been modified to become accessible to measurement. This concerns specially three points :

- the antireflecting treatment of the wall and blade surfaces
- the windows and their cleaning-device
- the possibility of local seeding

1. Surface treatment

Several criterions had to be respected :

- a compatibility with the materials to be treated (steel and titanium)
- a good temperature resistance (up to 150 °C)
- a good resistance to solvents used for cleaning
- a minimum additional thickness (because of the fineness of the blades)
- the necessity of treating the whole rotor without removing the blades (because of the mechanical equilibration)

The solution was founded with a particular mat black paint.

2. The sight windows and their cleaning device

Six different sight windows have been mounted on the shroud of the machine to have access to the compressor channel. A tangential view of their position is presented figure 2.

Some problems occurred in the stator because of the fixing of the blades : two blades had to be cutted and we had to control their vibration level.

- The window glasses being flat (mounted in a curved wall), we have minimized their size as much as possible : the glass diameter corresponds to a refracting light solid angle of 20 degrees when measurements are done near the hub.
- Each window is provided with a cleaning device which allows cleaning of the glass without stopping the machine (figure 3). The solvent (Toluene) is injected in a circular channel with a suitable pressure (depending of the local flow pressure). The liquid is convected on the glass by the stream after its passage through slots provided all around the window.

3. Local seeding (figure 4)

Generally, seeding is realized upstream the machine. But, in special cases (measurements near the hub for instance), there are not enough particules in the measurement volume. So, it can be interesting to seed the flow just upstream this measurement point. For that reason, we used a smoke probe mounted on a carriage which move radially and tangentially, in order to position the probe approximatively on the same streamline that the measurement point.

Comparisons are shown figures 5 and 6. The differences could be explained by the slots provided in the shroud to allow the tangential displacement of the probe. These slots disturb the flow near the wall and then alter the whole radial equilibrium in the channel. After they have been obturated, the results became in quite good agreement.

IV. THE T.F.V. ANEMOMETER

1. The optical arrangement (figure 7)

In the last version of the anemometer, the emitting and the receiving optical systems are mounted in a single tube, the rotation of the two spots of the measuring volume being performed by the rotation of the whole tube.

In a next version, the part of the optical arrangement composed of L5, L6, M1 and M2 will be replaced by a fiber optic. The main characteristics of the anemometer are :

- distance between the two spots : 500 μm
- incident beam solid angle : $\pm 5^\circ$.

- refracting light solid angle : $\pm 10^\circ$
- front focal length : 300 mm

2. The anemometer support (figure 8)

This support, light and stiff, allows the different movements which are necessary for :

- the alignment of the velocimeter optical axis with the measurement section,
- the measurement sequence : translation across the channel and rotation of the two spots.

3. The electronic system

A diagram of the whole electronic system is presented figure 9 (the hachured elements concern synchronized measurements inside the rotating blade row).

The signals delivered by the two photomultipliers are, after their passage through preamplifiers and filters, directed towards the main part of a dual-counter specially studied and built for this purpose. Its resolution of 10 ns permits measurement of flow velocities up to 500 m/s with an accuracy better than one percent. The informations are then transmitted to the calculator which realizes acquisition, storage and reduction of the data.

4. The synchronized measurements

Two problems have to be solved during measurements inside a rotating blade row :

- the cancelling of the light refracted at each blade passage on the measurement volume,
- the determination of the azimuthal position of each information during the acquisition sequence.

The first problem leads to an overload of the photomultipliers and at a great amount of wrong measurements (the blade passage frequency is, in our case,

about 10 kHz). The solution is found in switching off the laser beam during the blade crossing, using a Pockel cell driven by an electric signal delivered by a synchronized wave-shaper. This wave-shaper treats the signal of a photoelectric cell mounted on a slotted disc (the number of slots being the same than the number of blades -figure 10). The adjustment procedure of the wavelshaped signal is presented figure 11 : the width and the delay of the signal are set to coincide with the blade crossing signal. Then, the Pockel cell cancels this blade signal.

The second problem is solved in using the secondary part of the dual-counter (1 μ s resolution). The reset of this counting system is performed by the wave-shaped signal (i.e. the passage of each blade), and the latch by the start photomultiplier signal. A procedure, described in figure 12 and 13, inhibits all possibility of a new measurement during the transit time of the two informations (velocity and azimuthal position) from the counter to the calculator.

V. OTHER ENCOUNTERED PROBLEMS

We have already mentionned problems relative to seeding and cleaning. Another problem, connected with the specific surrounding, is the one of the eddy currents due to the 600 kW electric driving-motor : for that purpose insulation and screening must be done with carefulness.

Other problems that are encountered near the wall, where a lack of particules is observed, and specially in the rotating blade row will be discussed now.

1. Near the shroud, the windows get dirty very rapidly because of the crushing of the particules on the glass. This phenomena, very important with a reduced leakage, disturbs mainly the measurements near blade tip.
2. Near the hub, a part of the blade passage near the suction side is not accessible to the laser beam. This "mask effect" is due to the twisted form of the blades and can cover up to 40 % of the blade passage (figure 14). A possible solution is to explore oblique sections.
3. This "lost region" is enlarged by the particular geometry of the blades at their junction with the hub (arrow on the figure 16) which forbids measurements in this region.

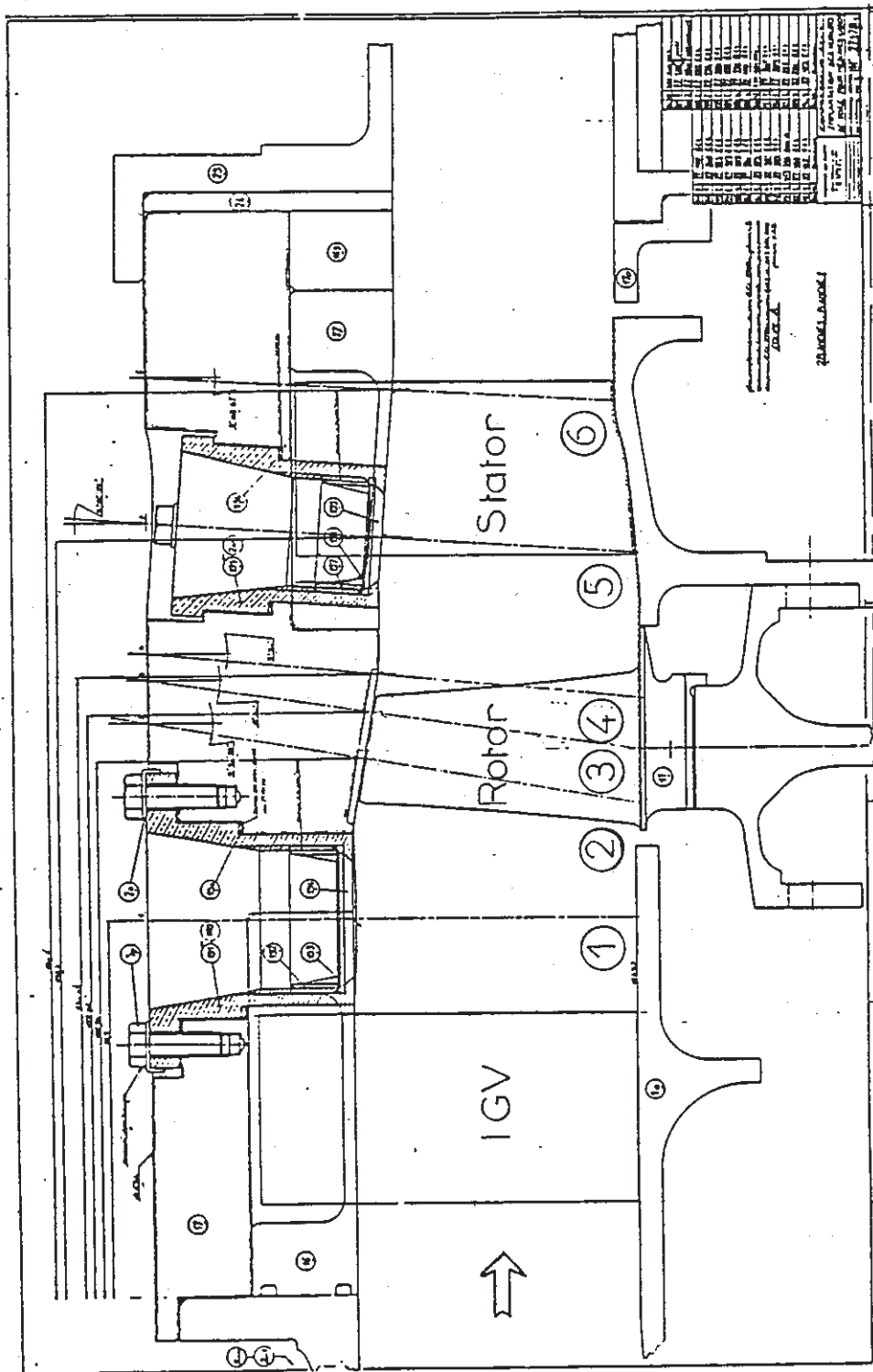
4. Another problem comes from the fact that the laser beam axes are perpendicular to the shroud and consequently not normal to the hub. Then, all the particles velocity vectors are not contained in the focusing plane of the front lens and the validity rate of the measurements is reduced (figure 15).

5. The ratio between the blade passage g and the blade height h is rather small in our case (figure 16). That leads to a solid access angle at the hub, lower than 20 degrees in the best case (at mid-passage). This decreases the refracting light level recovered by the photomultipliers. Further, it can affect the incident light solid angle and distort the measurement volume.

All these phenomena lead to a reduced validity rate and an increased acquisition time.

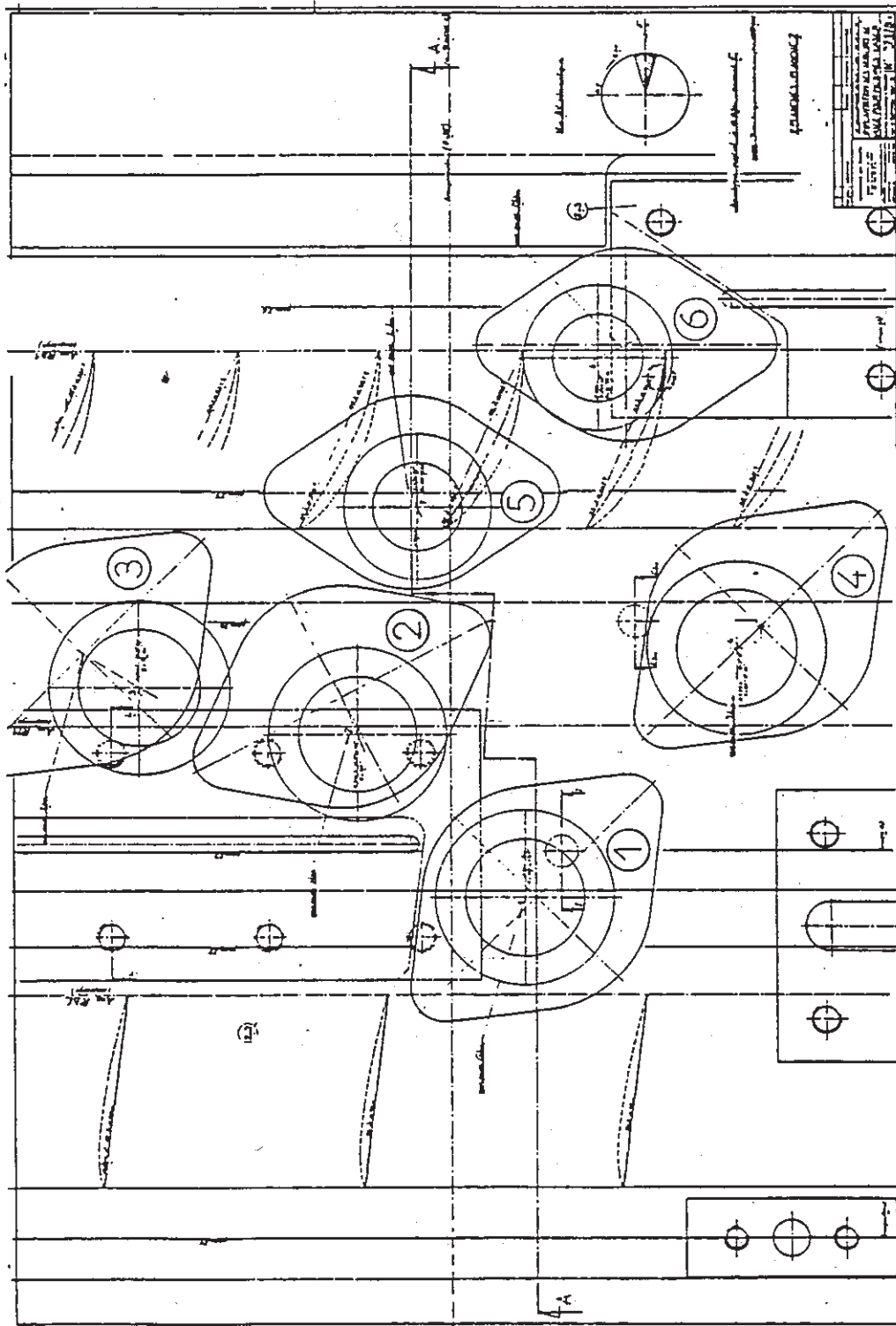
VI. SOME MEASUREMENTS

- Some examples of reduced velocity V/U and absolute angle α azimuthal evolutions, for different points inside the rotating blade passage, are presented figures 17, 18 and 19.
- A comparison with inviscid calculation results is shown figure 20.
- Two examples (concerning meridional velocity V_m and relative angle β) of blade passage iso-values maps are also presented figures 21 and 22.



Six Measurement Sections

Figure 1



Windows Position

Figure 2

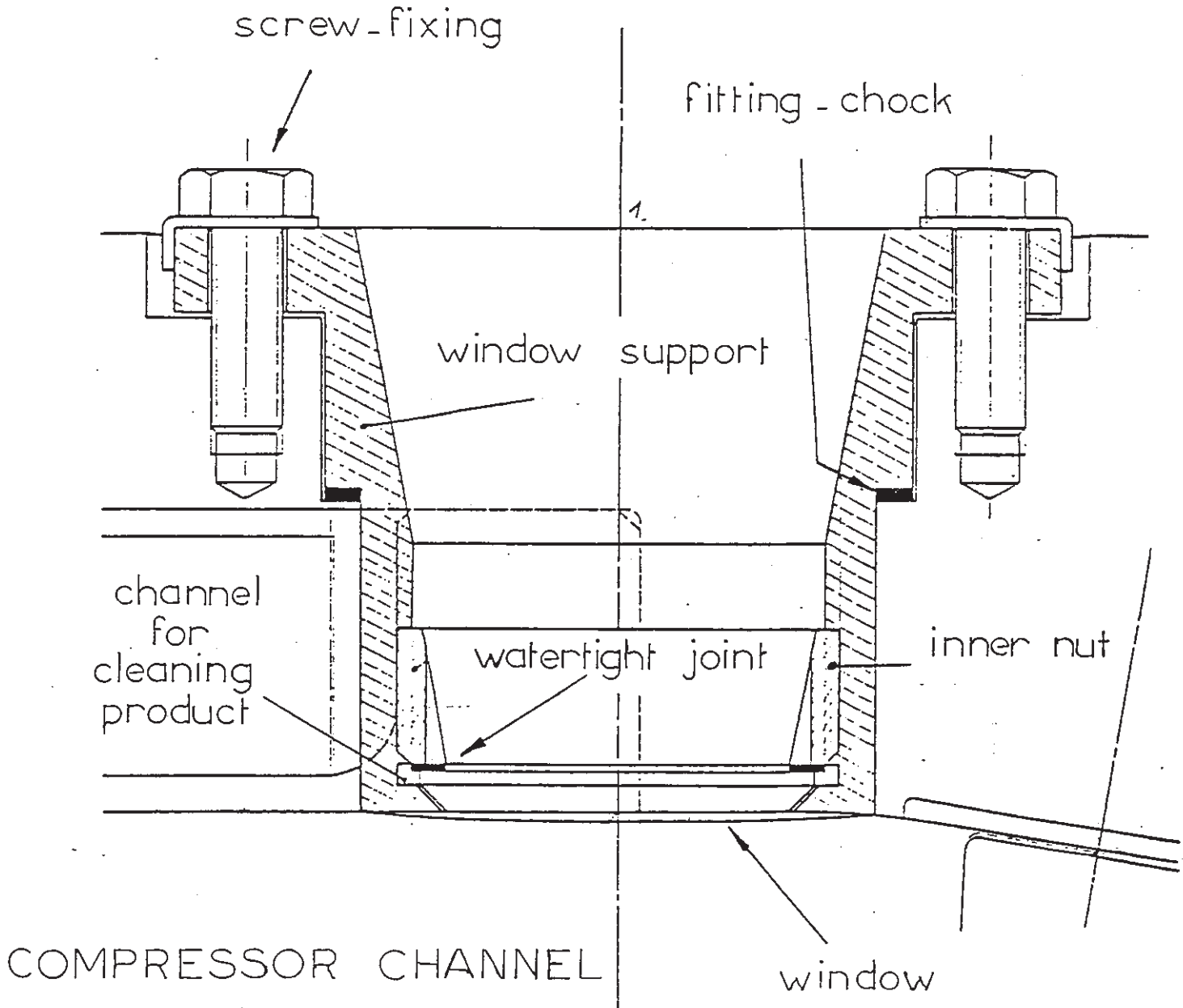
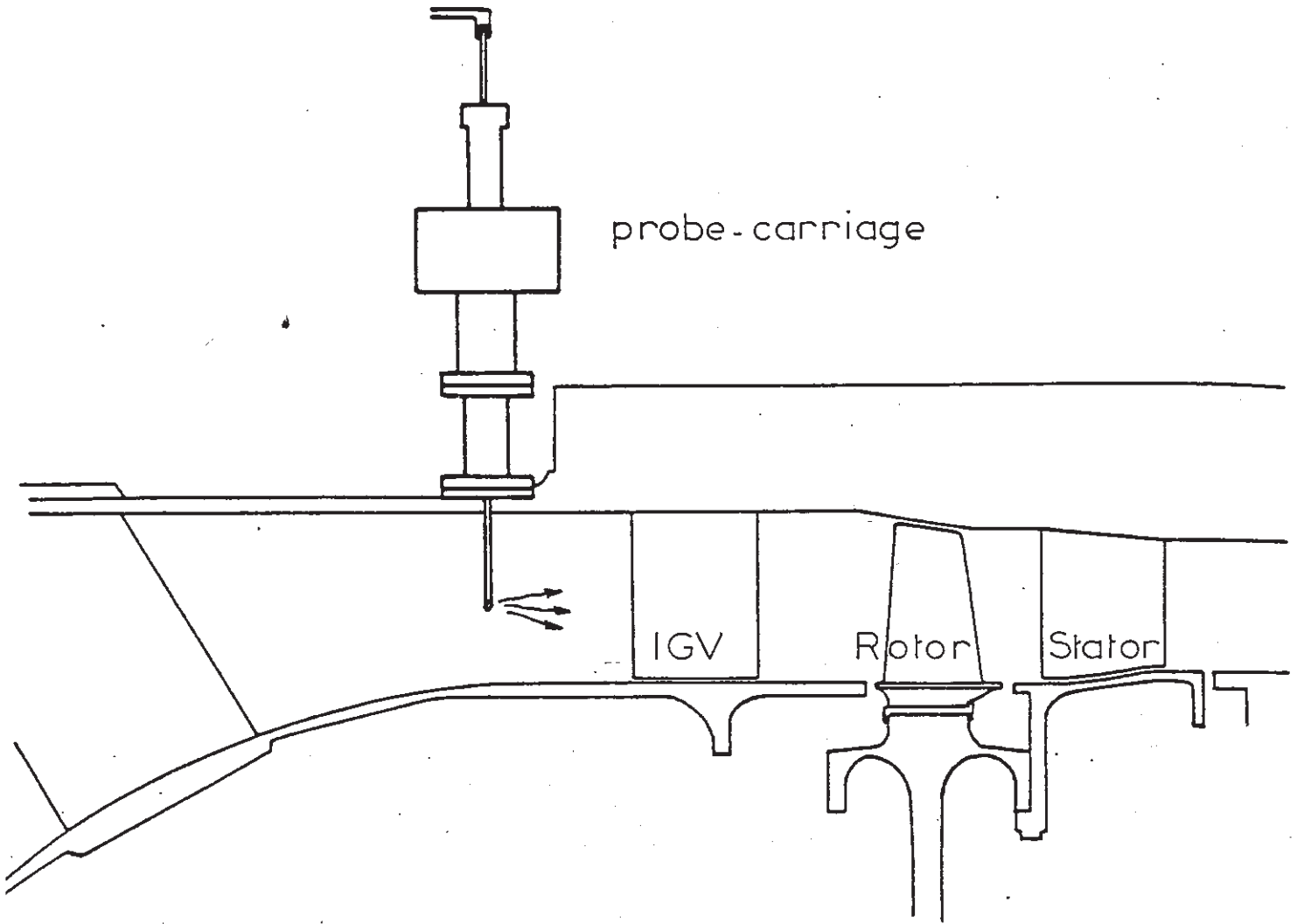


Figure 3



Position of the Smoke-probe

Figure 4

section 5

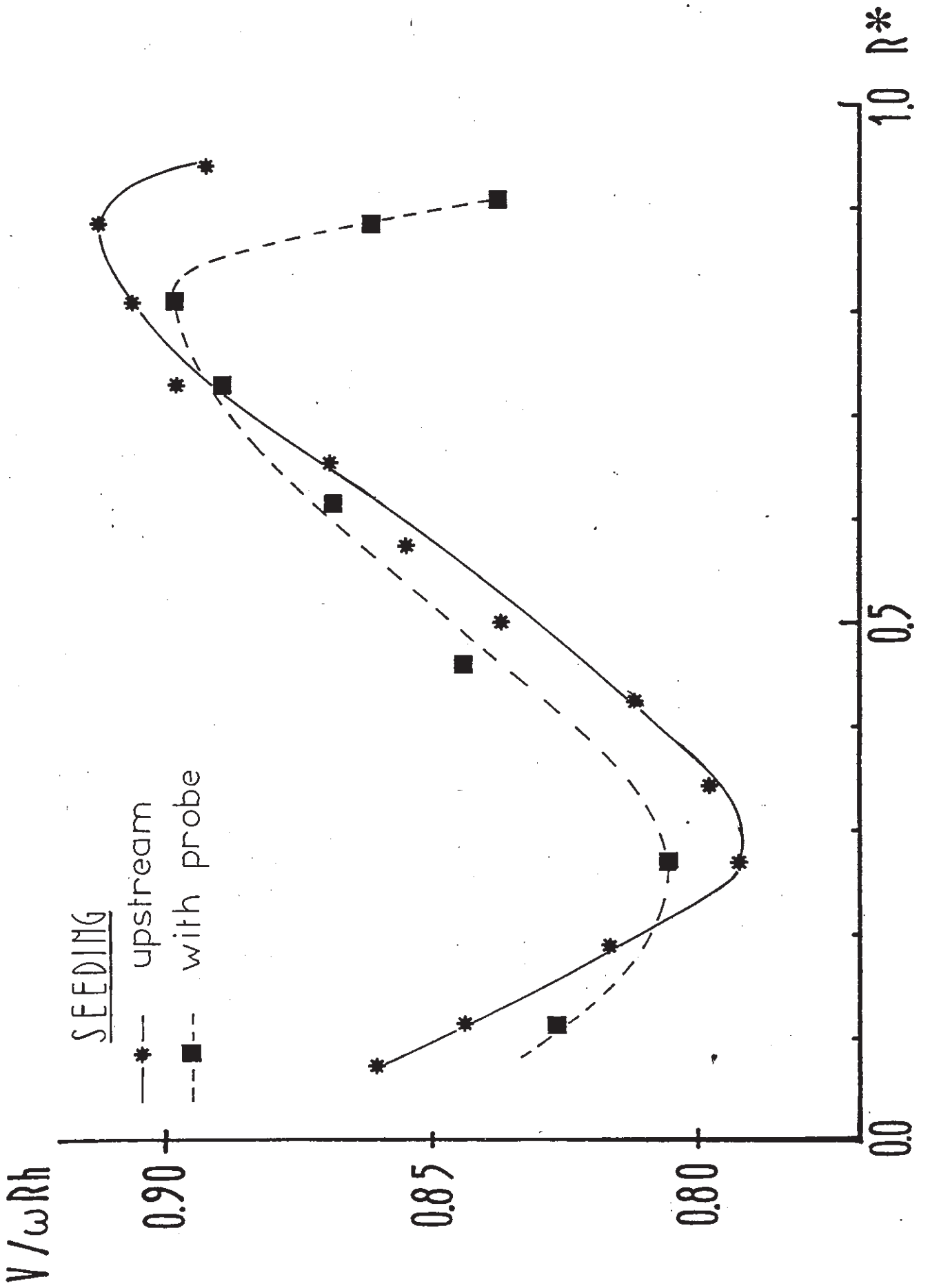


Figure 5

section 5

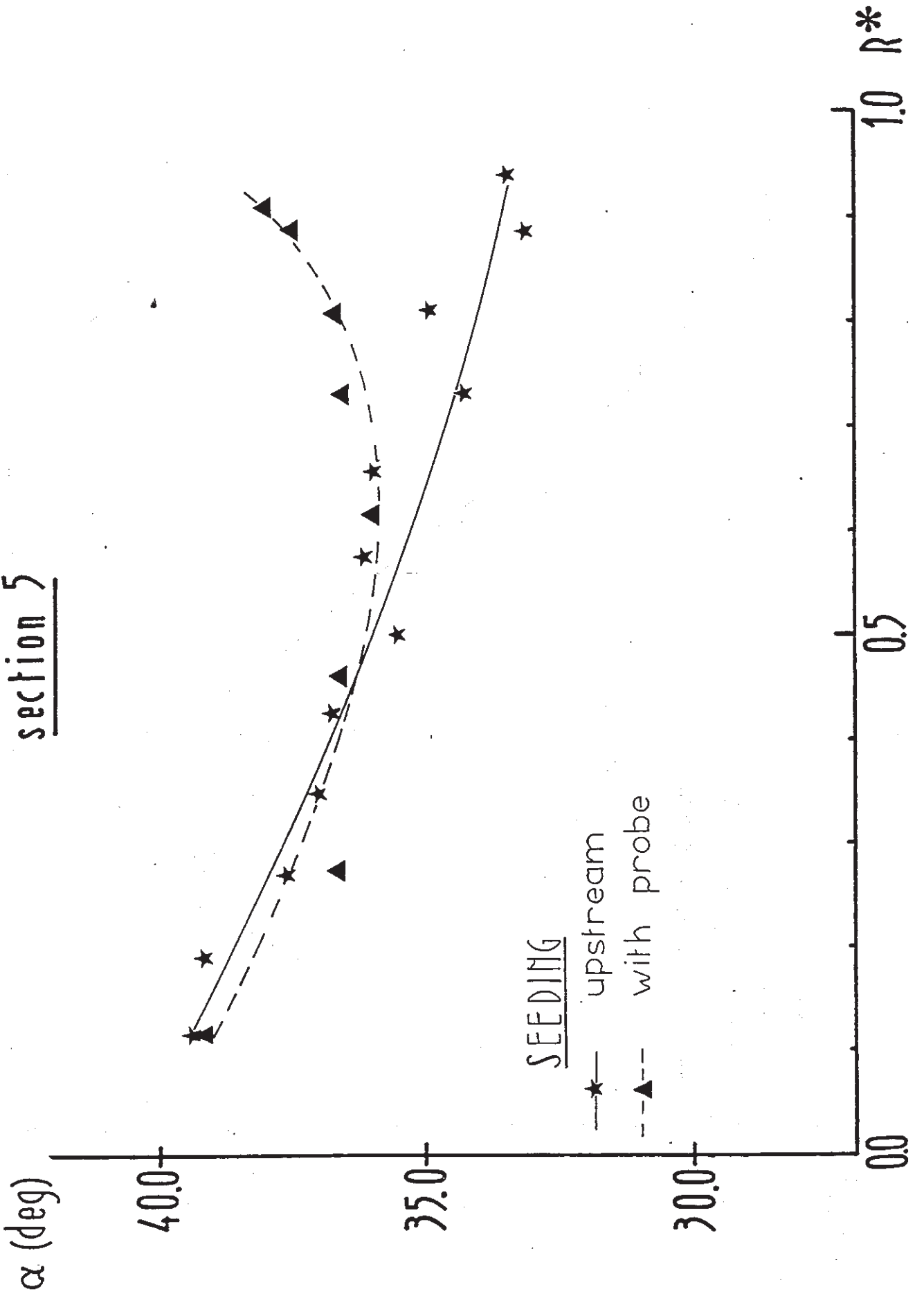
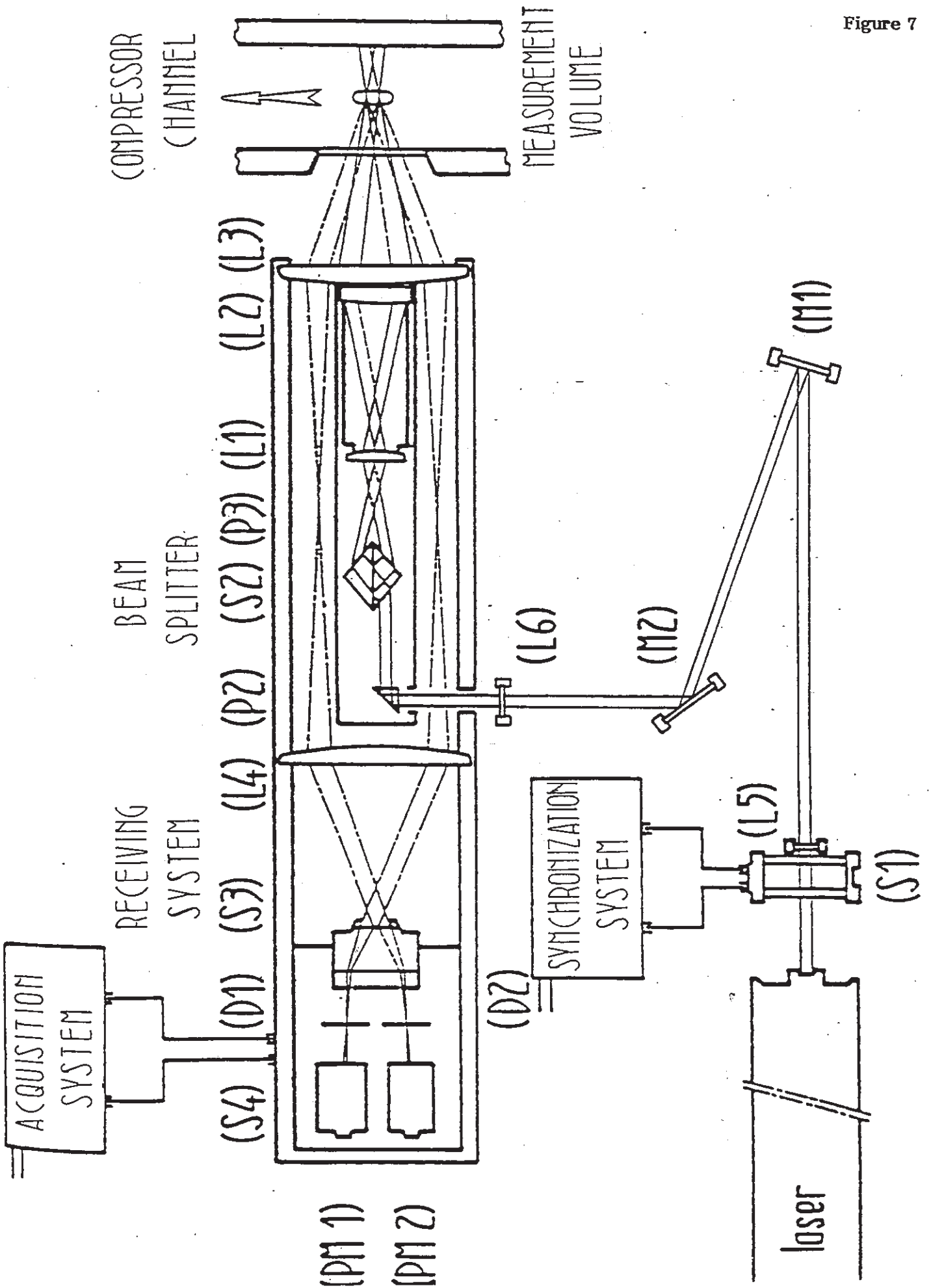


Figure 6

Figure 7



Anemometer Support

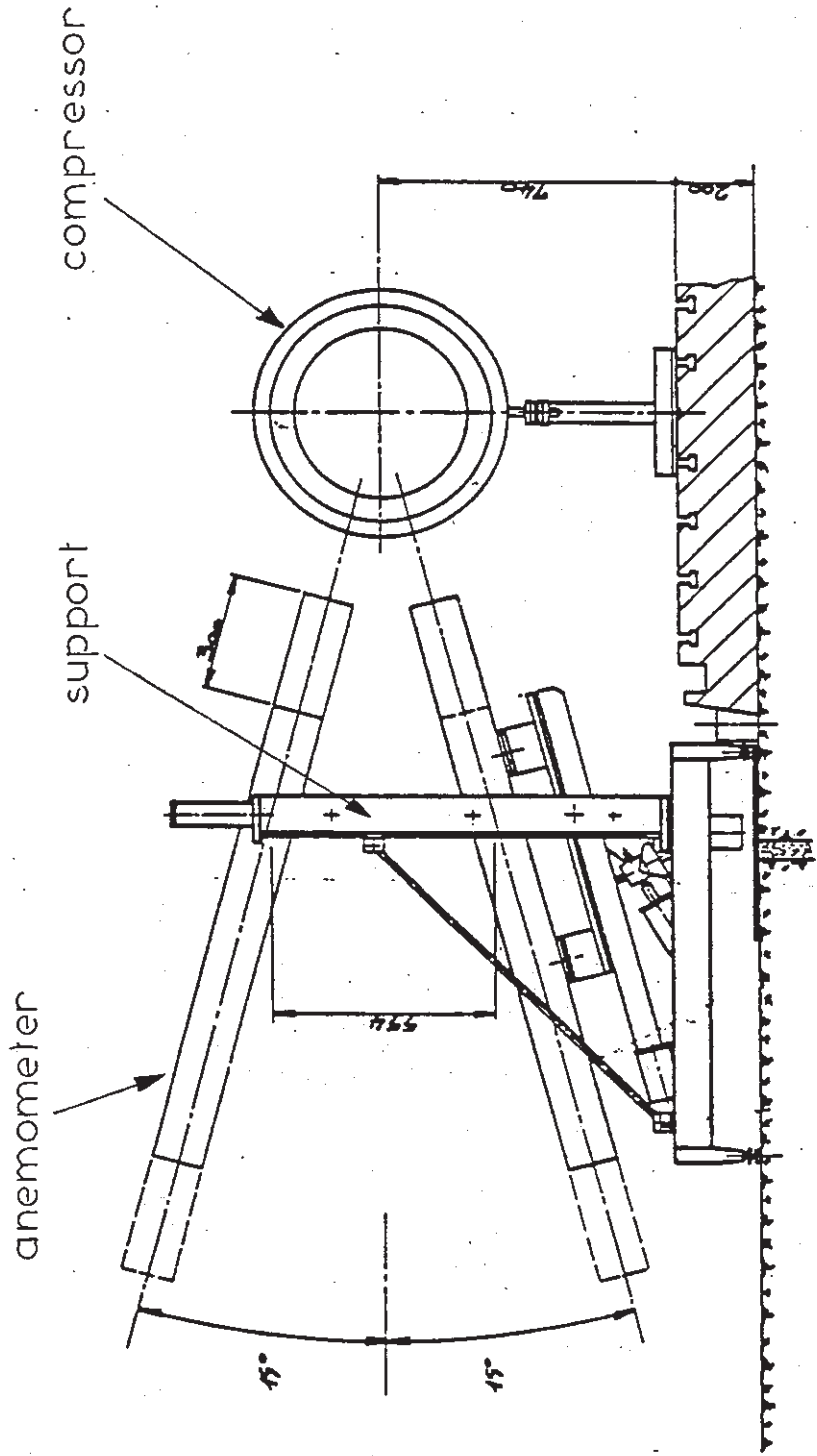
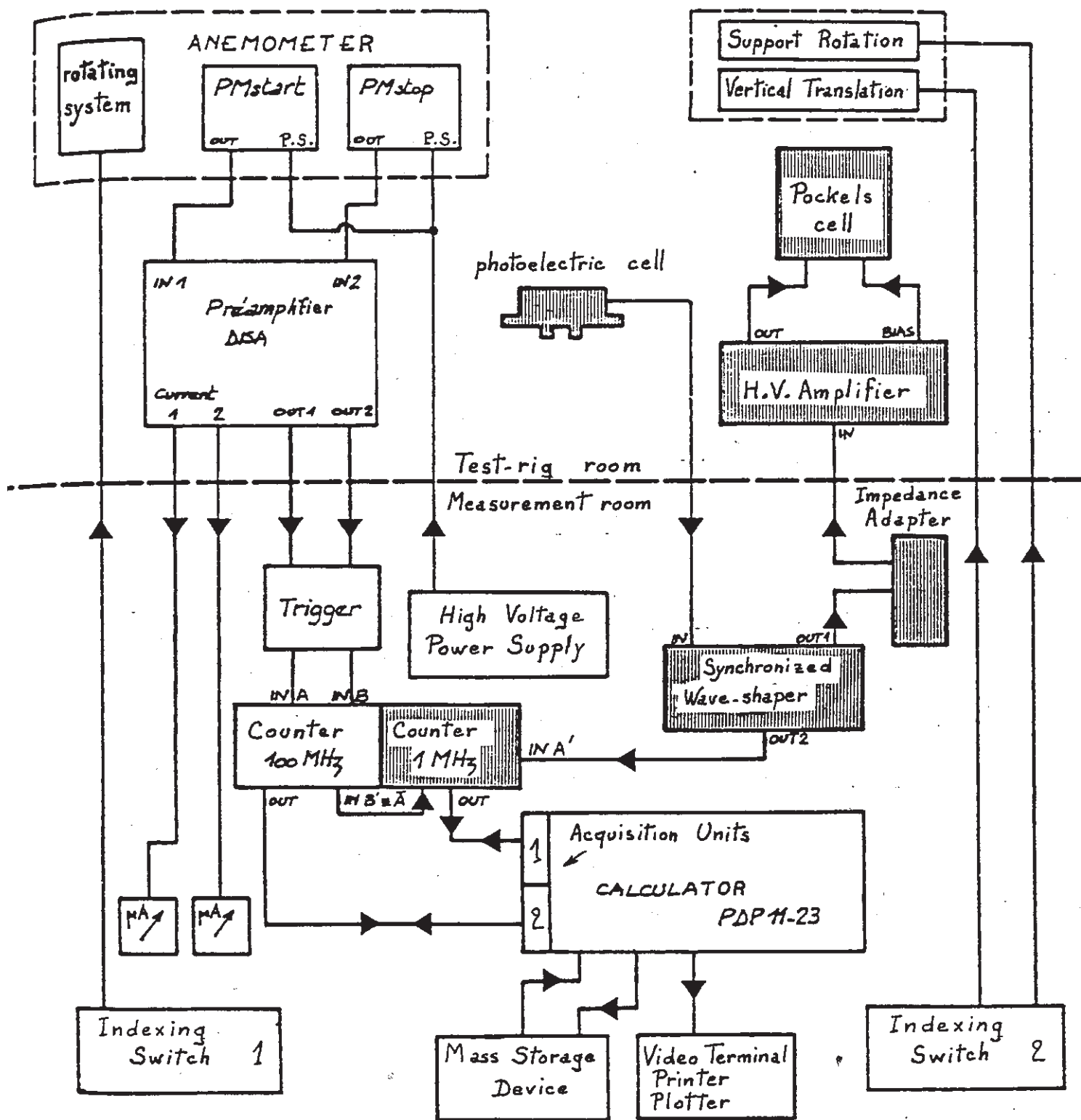
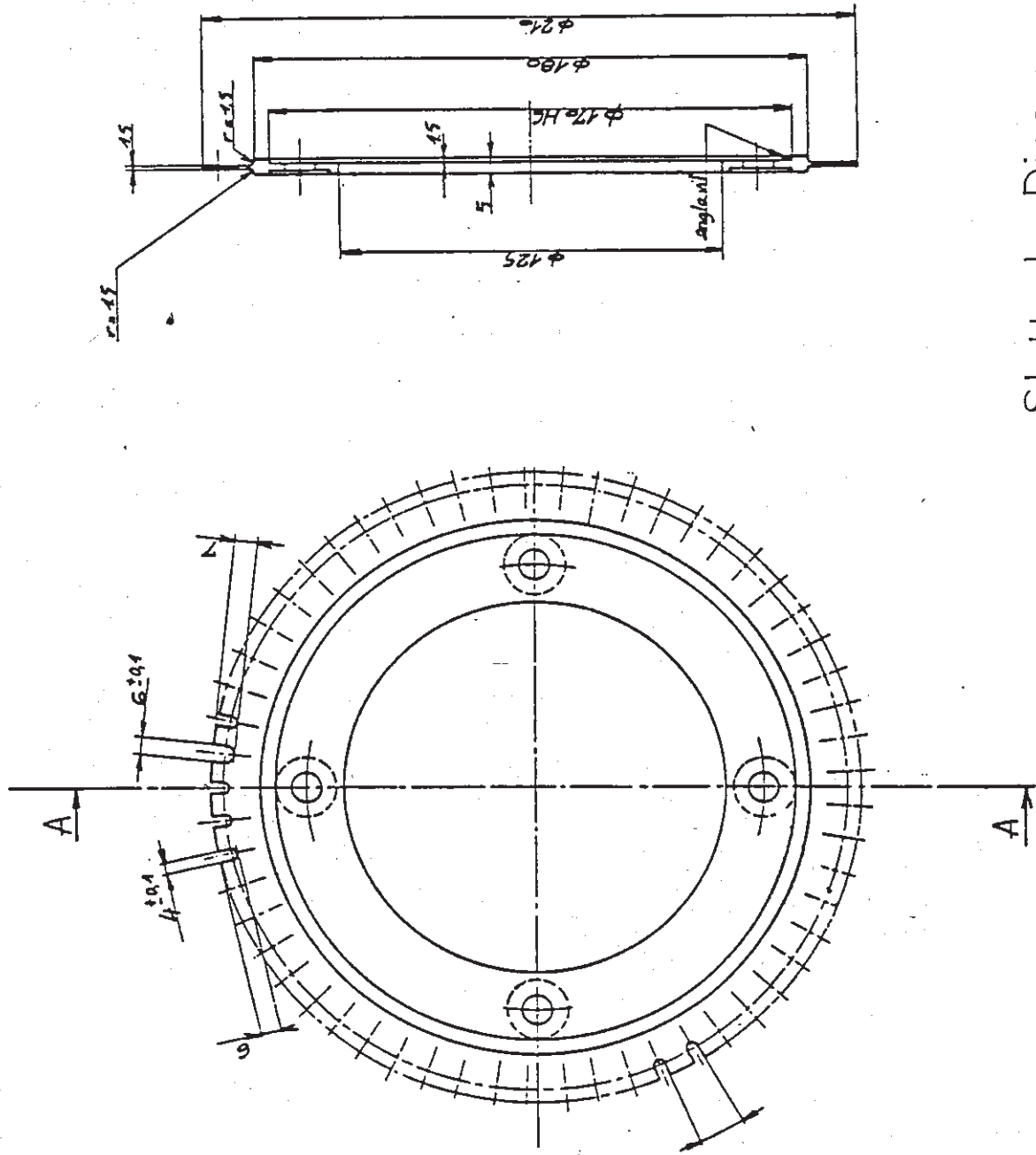


Figure 8



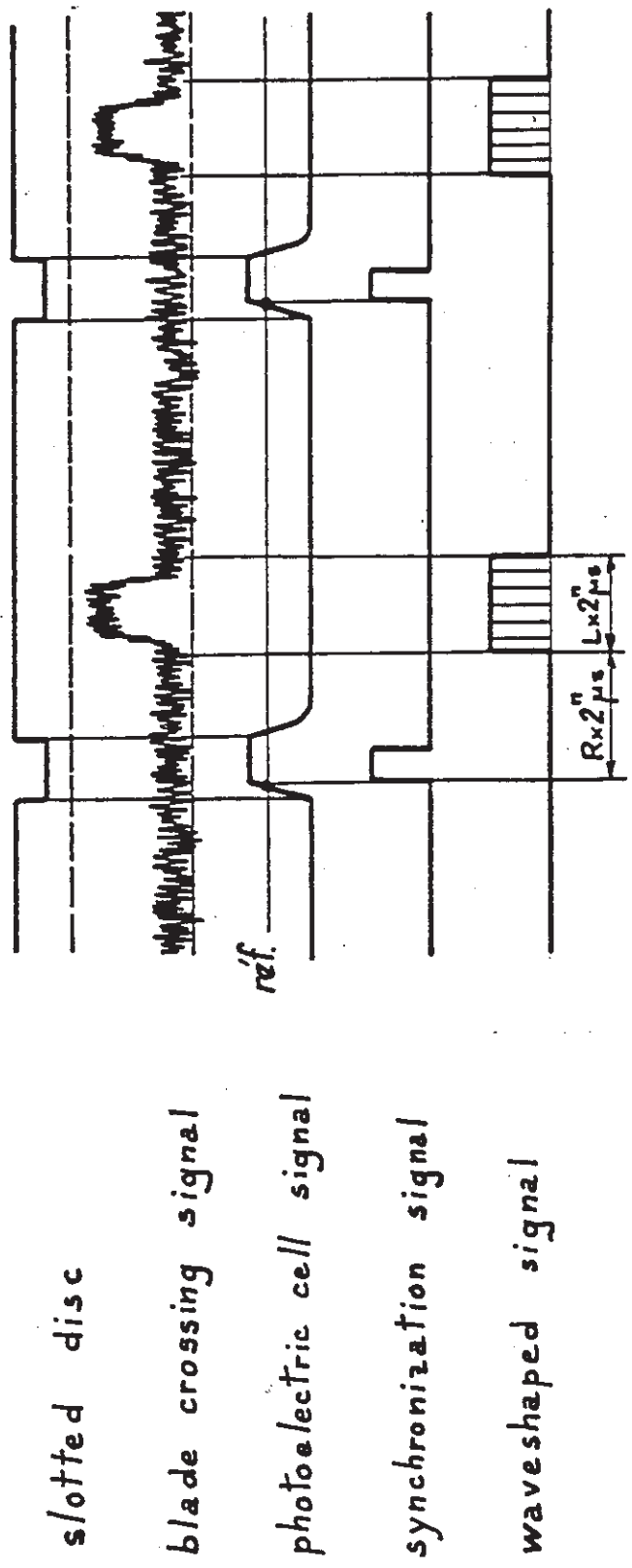
Synoptic Scheme of the Electronic System.

Figure 9



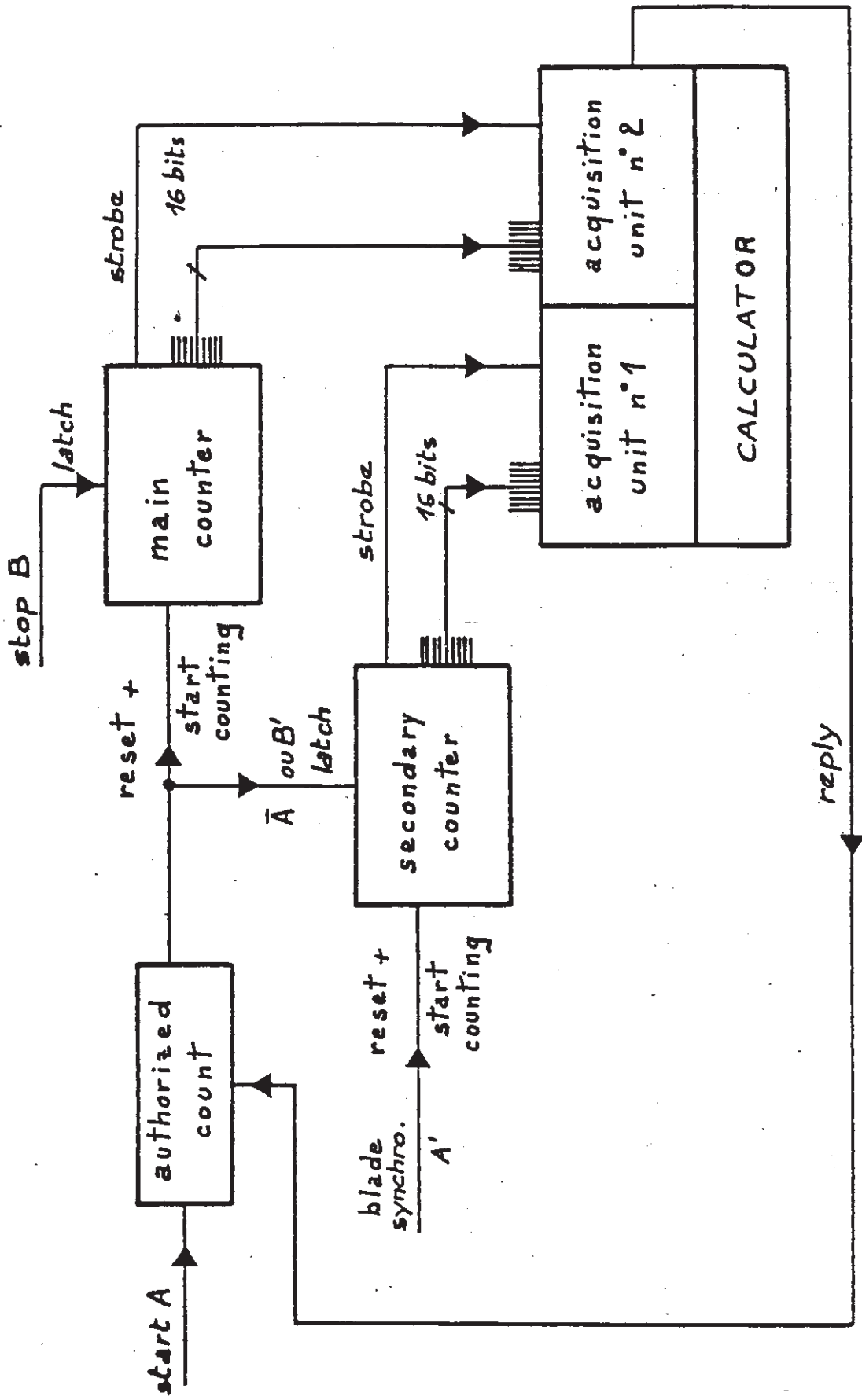
Slotted Disc

Figure 10



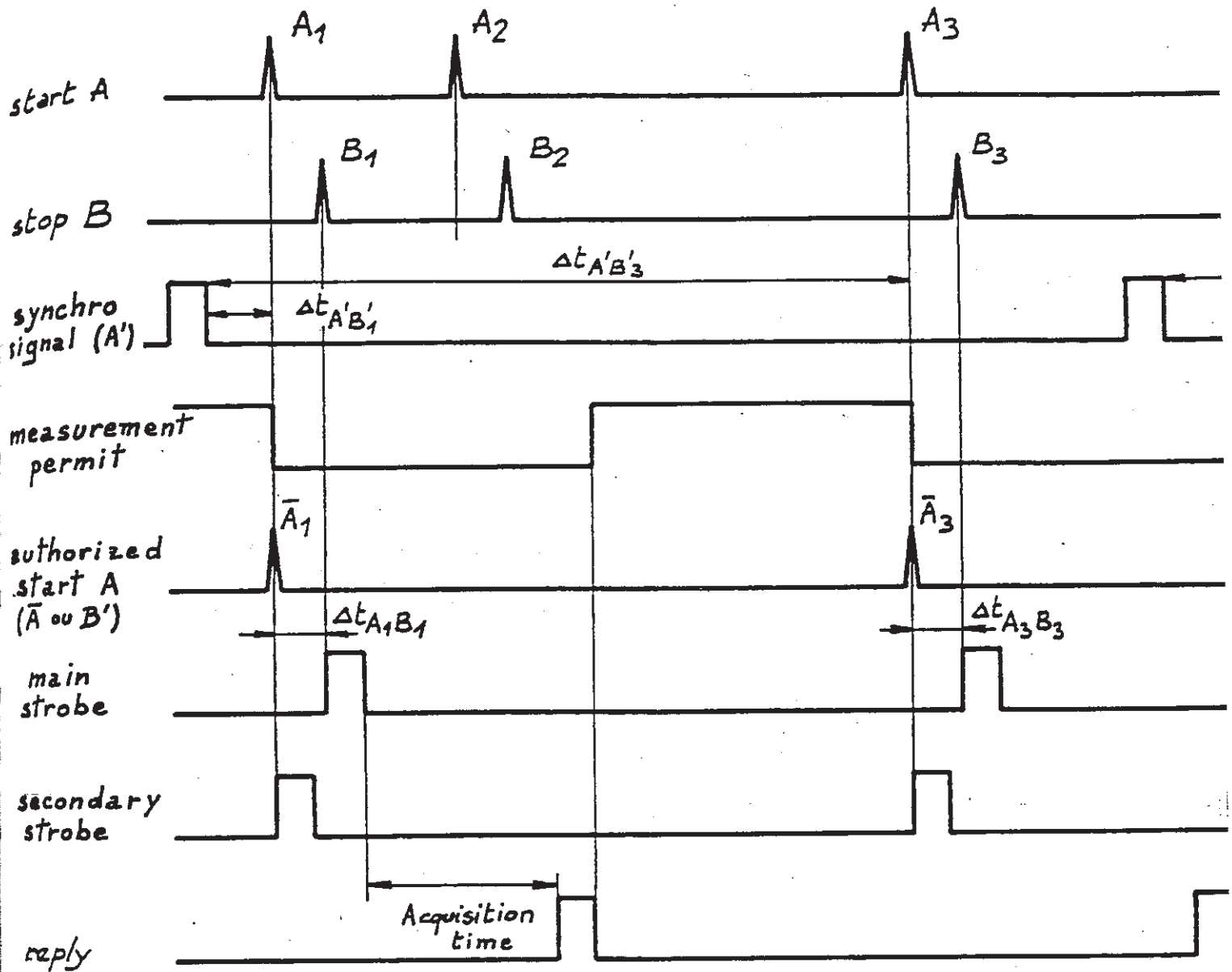
Synchronisation Signals Characteristics

Figure 11



Synoptic Scheme of the Synchronization System

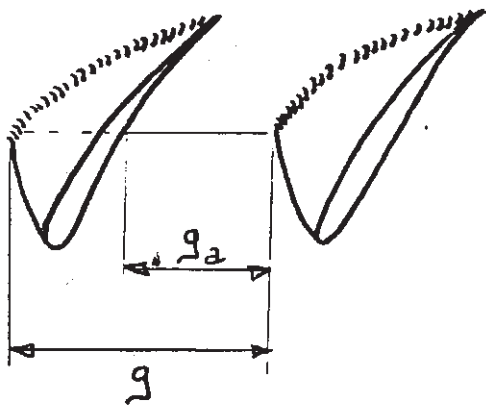
Figure 12



Acquisition. Procedure for Synchronized Measurements

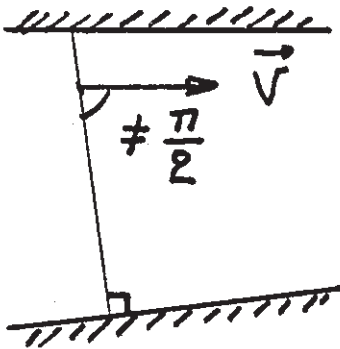
Figure 13

Figure 14



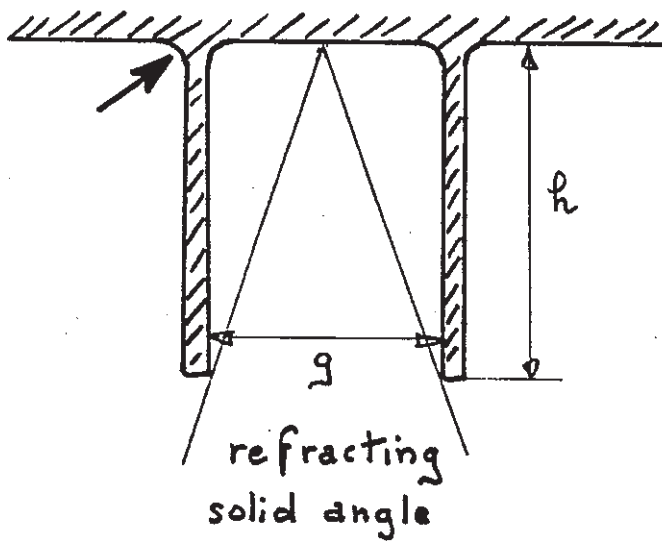
Mask effect

Figure 15



Direction of the measurement section

Figure 16



Aspect ratio of the blade passage

section 3

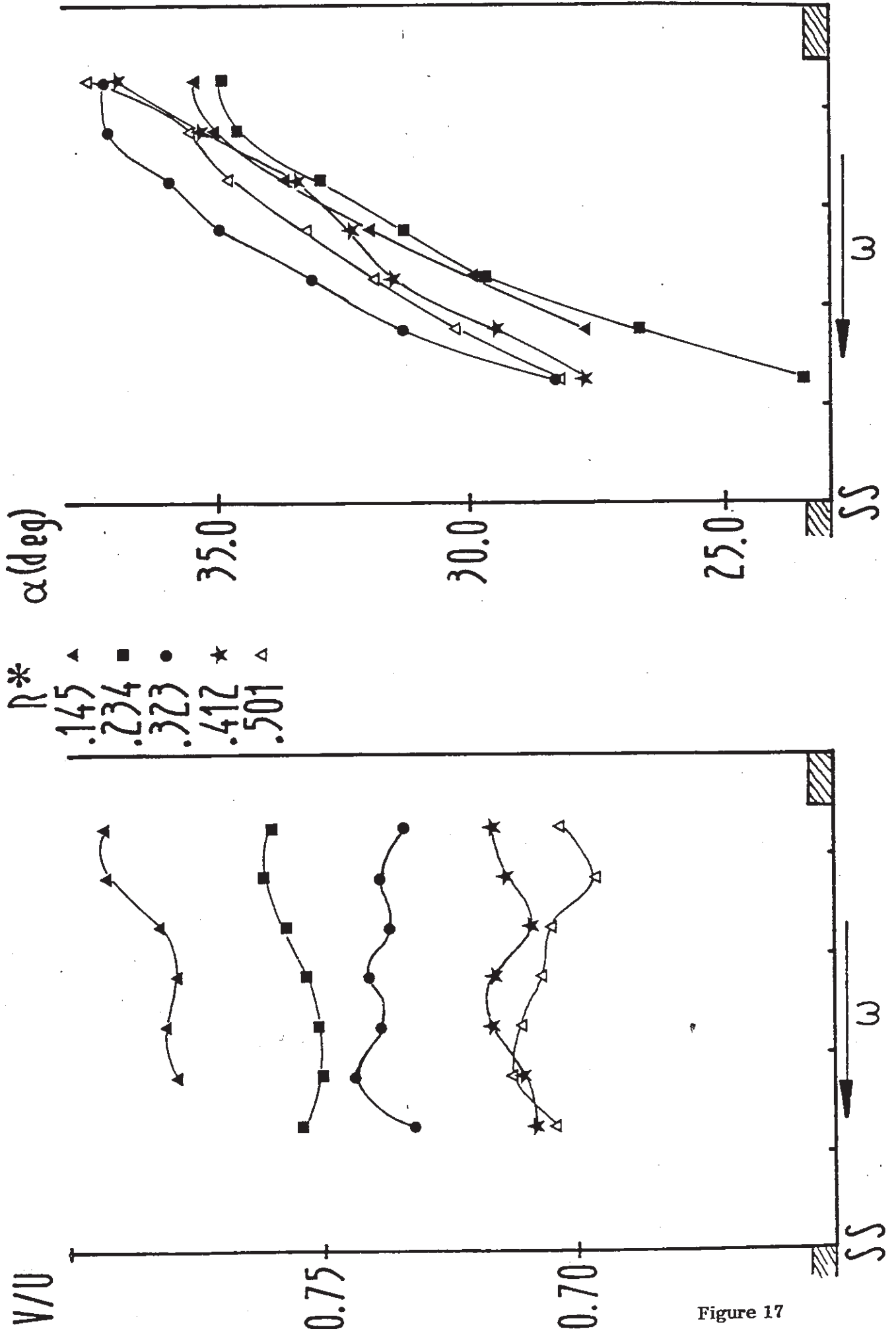
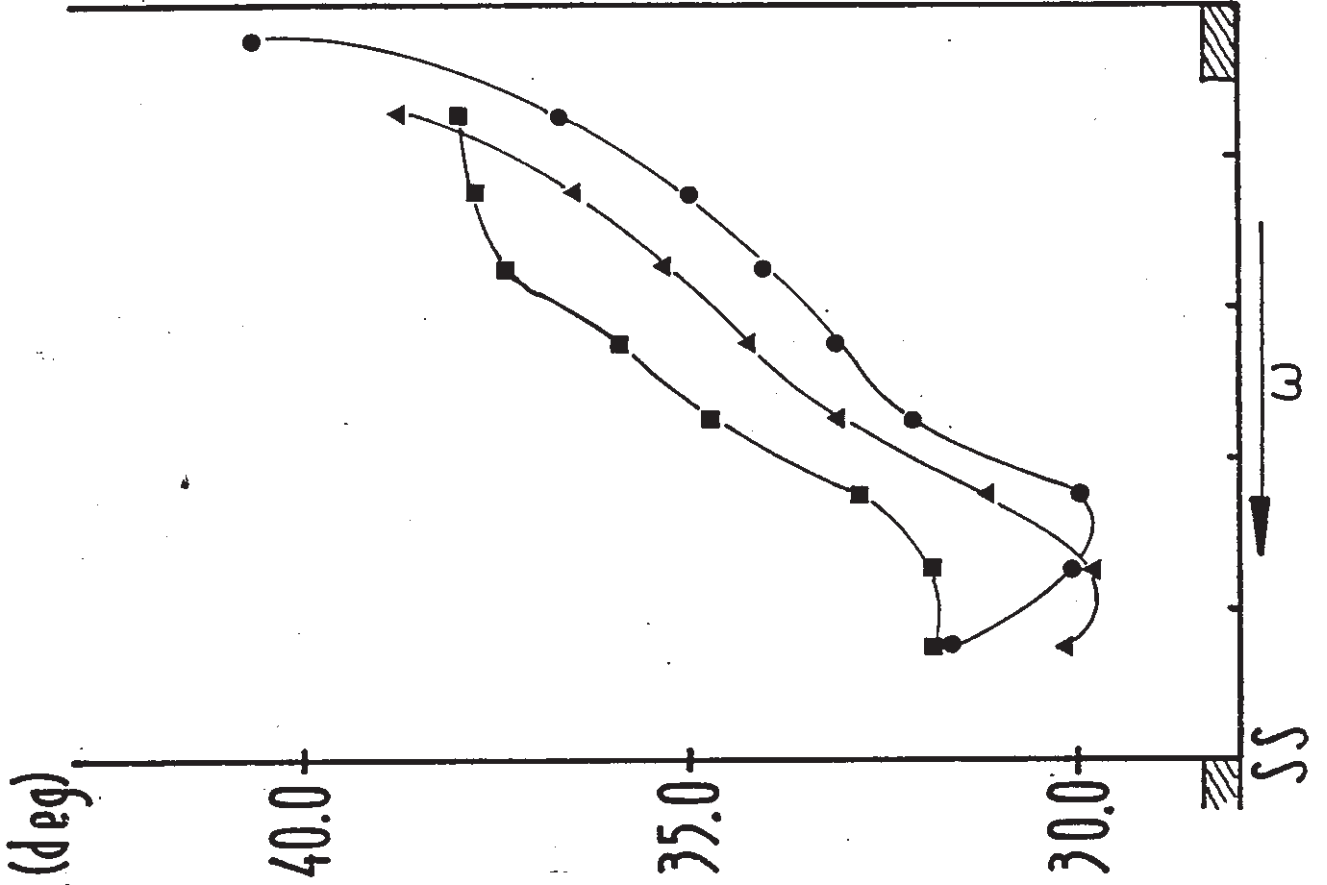


Figure 17

section 3



R^*
▲ .590
■ .679
● .768

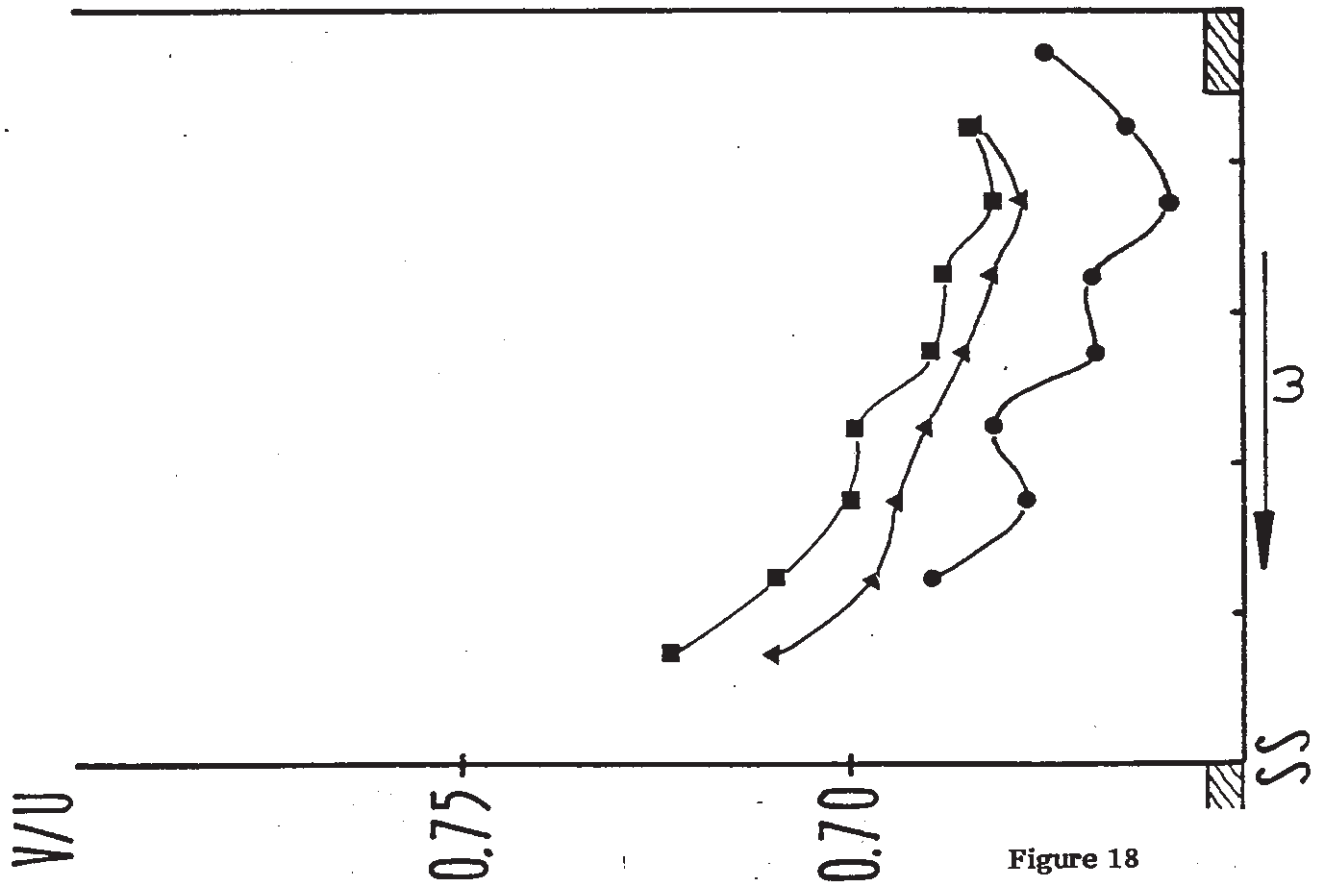


Figure 18

section 3

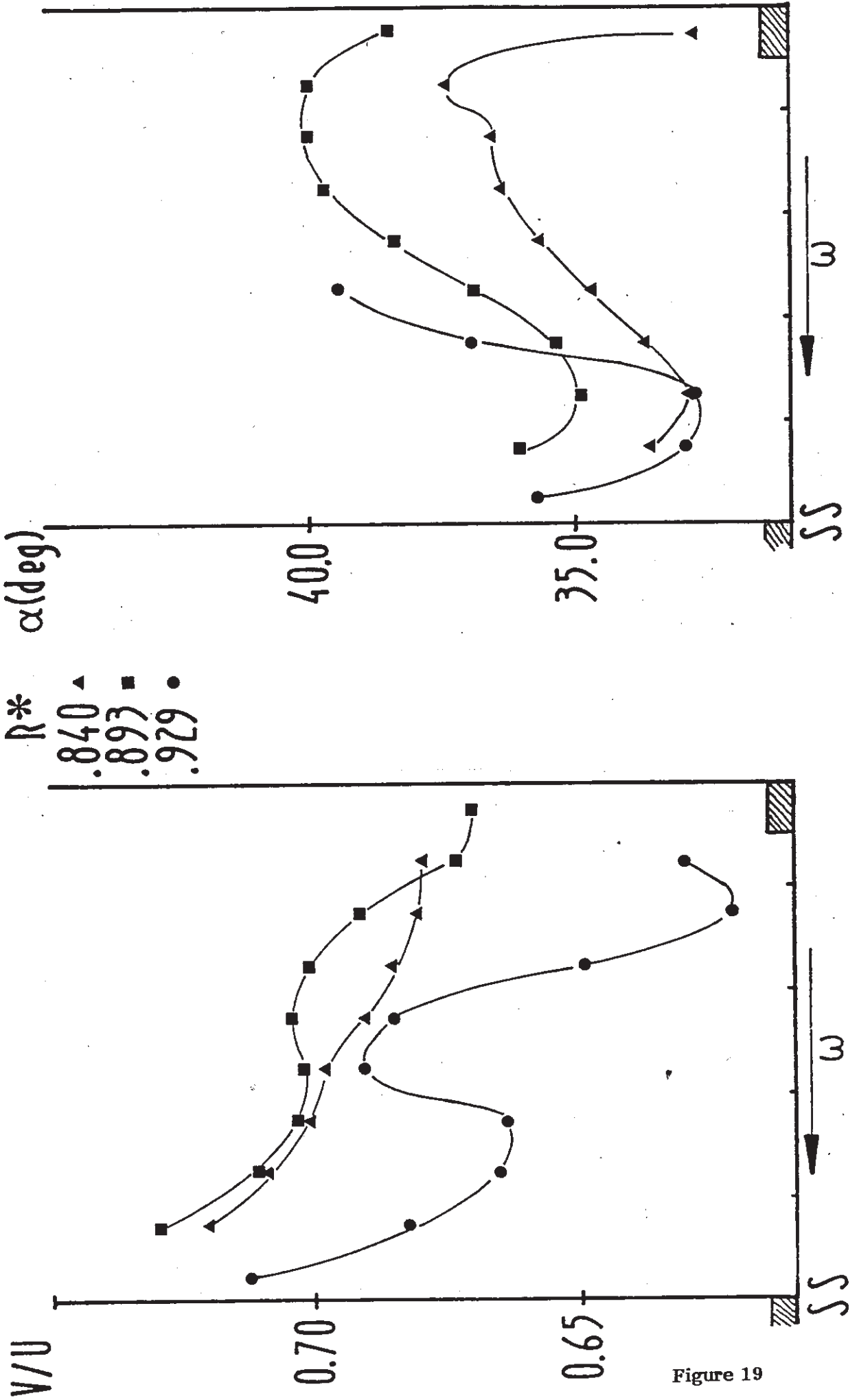


Figure 19

section 2 h=.75

Wm/U

* T.F.V.

— calculation

0.6

0.5

SS

PS

section 3 h=.75

Wm/U

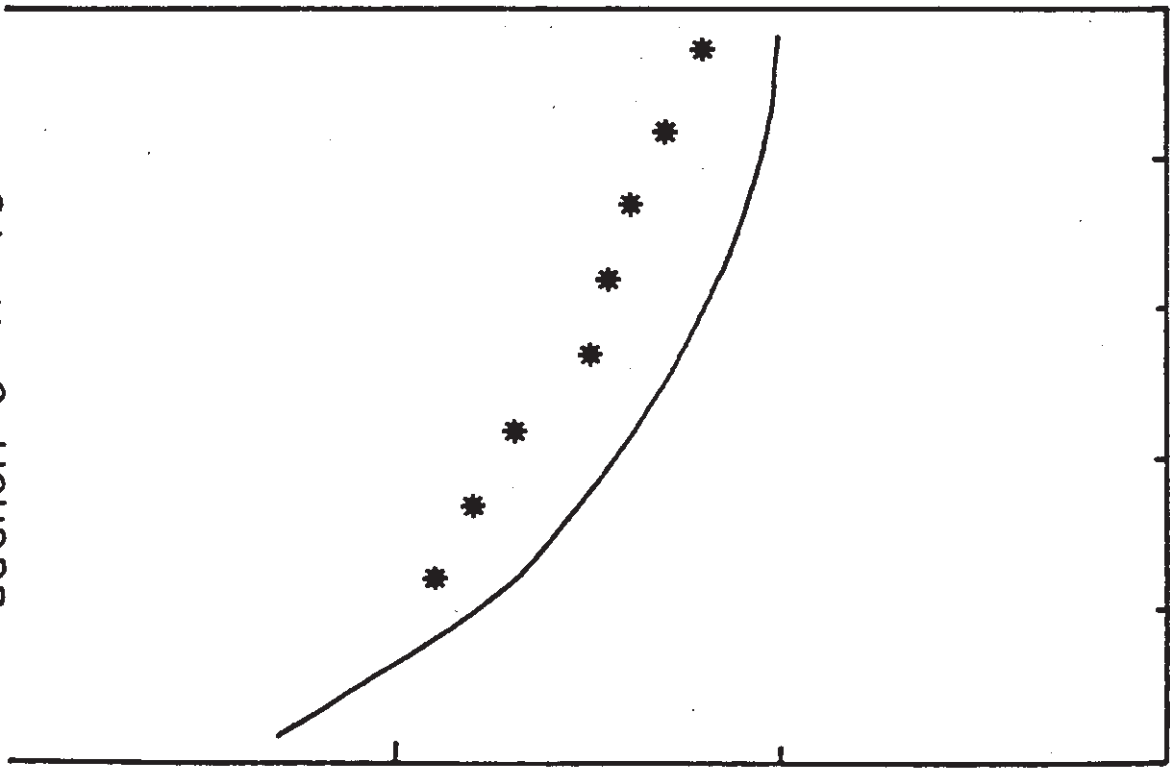
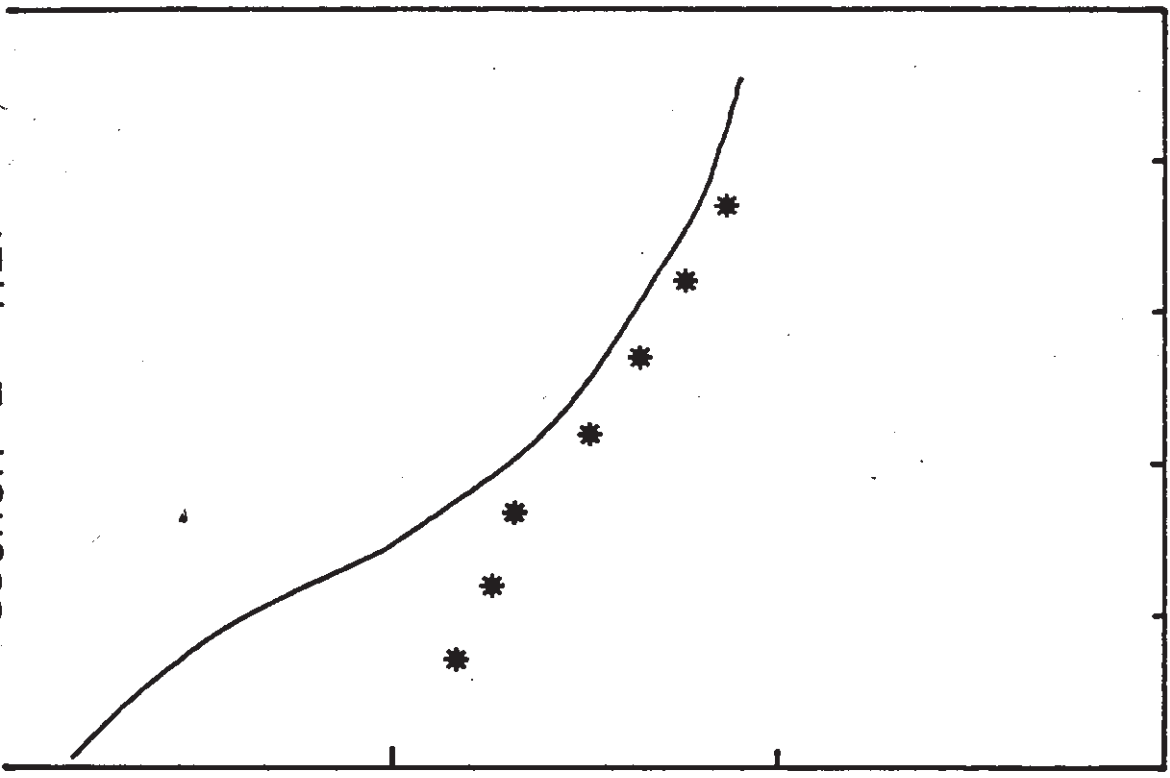
0.6

0.5

SS

PS

Figure 20



136.0 \$
140.0 +
145.0 x
150.0 o
155.0 *
160.0 Y
165.0 @
175.0 &
178.0 \$

Vm section 3

shroud

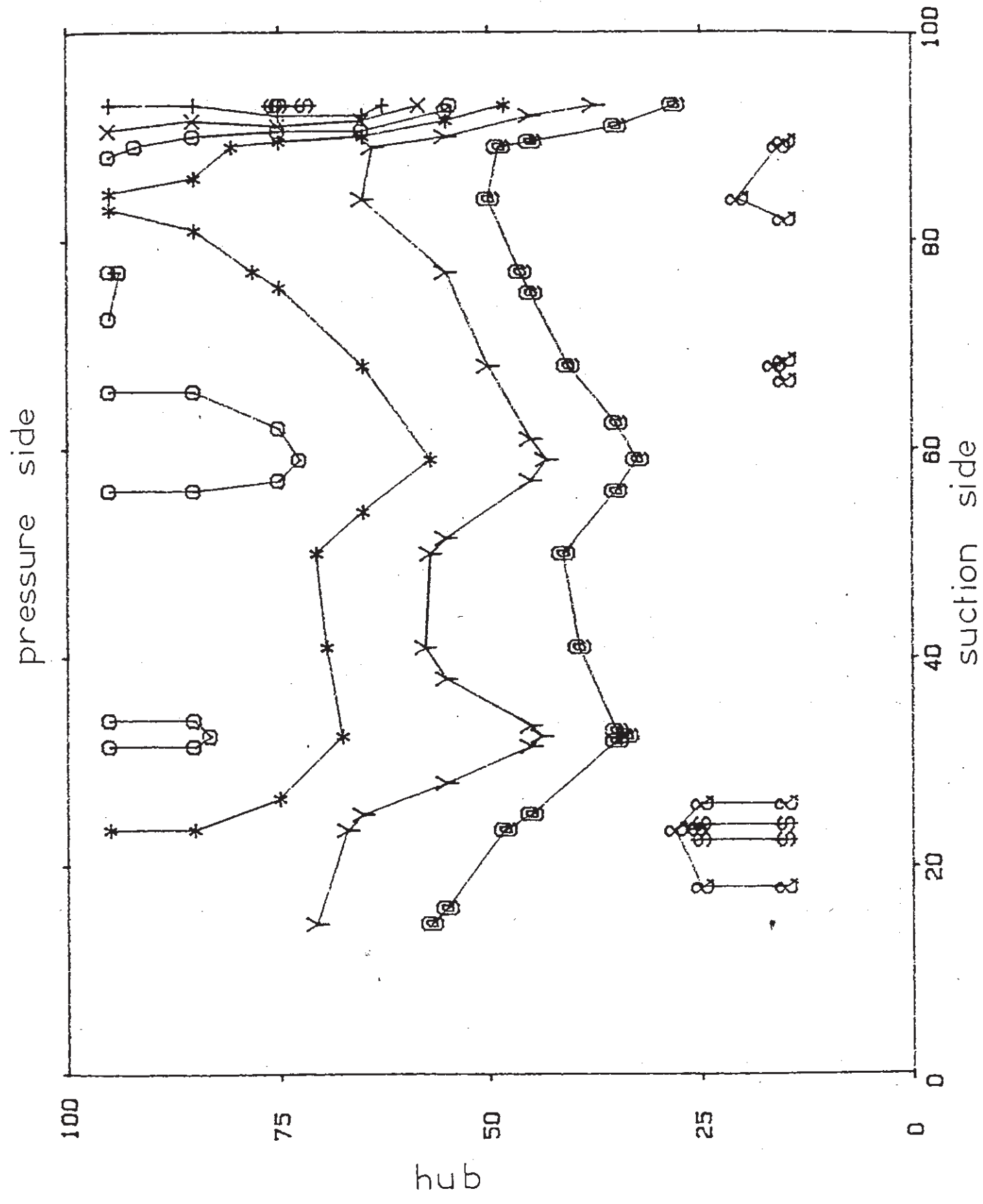


Figure 21

39.0 \$ + x o * Y o
 41.0 + x o * Y o
 43.0 x o * Y o
 45.0 o * Y o
 47.0 * Y o
 49.0 Y o
 51.0 o

β section 3

shroud

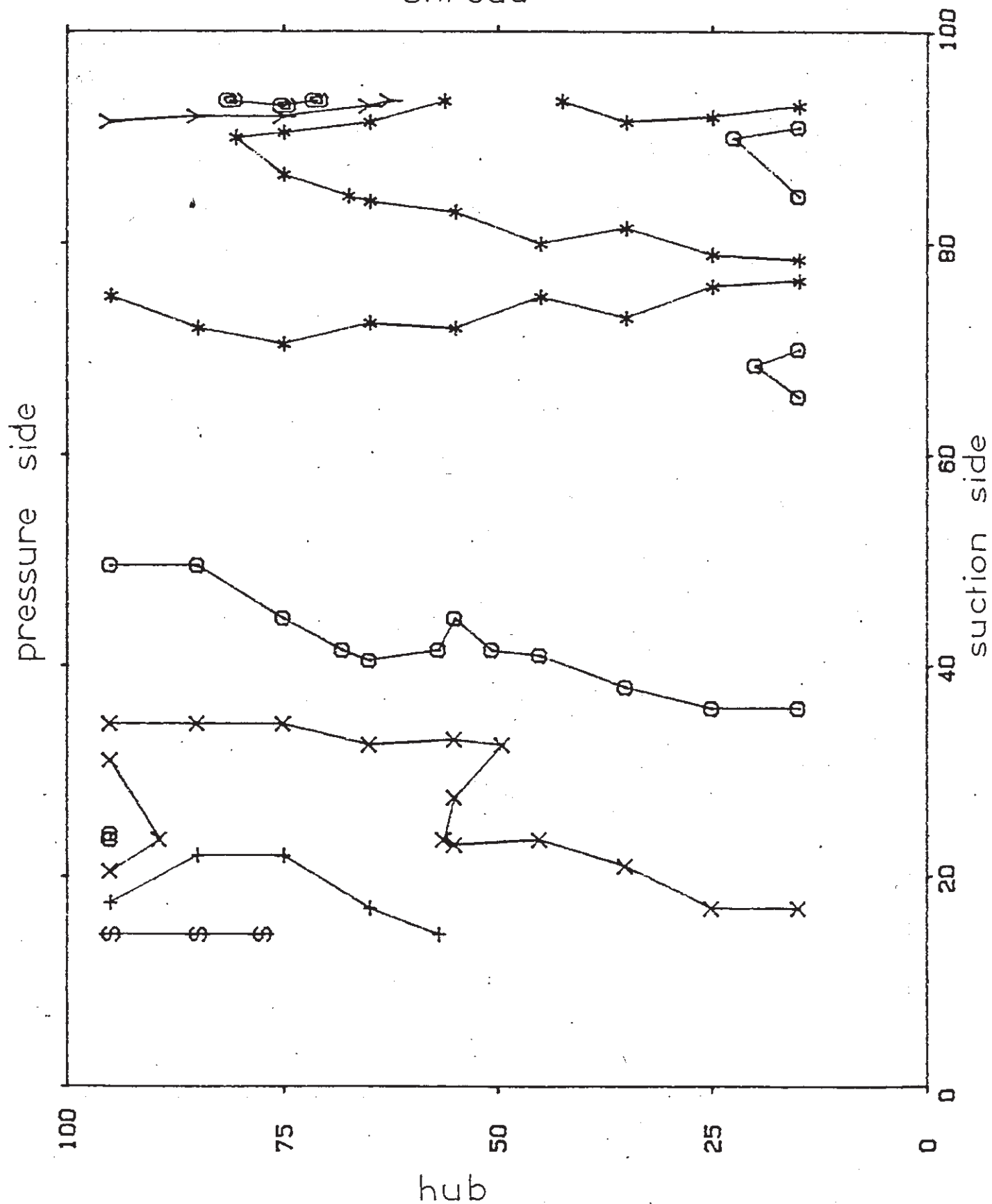


Figure 22